Monthly Notices
of the
ROYAL ASTRONOMICAL SOCIETY

MNRAS **483,** 4884–4892 (2019) doi:10.1093/mnras/sty3361

A photoionization model grid for novae: estimation of physical parameters

Anindita Mondal,[1]★ Ramkrishna Das,[1] Gargi Shaw[2] and Soumen Mondal[1]

[1]*S. N. Bose National Centre for Basic Sciences, Salt Lake, Kolkata 700 106, India*
[2]*Tata Institute of Fundamental Research, Mumbai 400 005, India*

Accepted 2018 November 6. Received 2018 November 5; in original form 2018 June 26

ABSTRACT

We present a method to estimate the physical parameters of nova systems using an extensive grid of photoionization models for novae. We use the photoionization code CLOUDY to construct a grid of models covering a wide range of parameters, for example the total hydrogen density ($n_{\rm H}$), the source temperature ($T_{\rm BB}$) and luminosity (L), the inner radius ($R_{\rm in}$) and the thickness of the ejecta (ΔR), keeping other elements other than hydrogen at solar values. In this way, a total of 1792 models were generated. From the model-generated spectra, which cover a wide wavelength region from the ultraviolet to the infrared, we calculate the ratios of hydrogen and helium emission-line fluxes, which are generally strong in nova spectra. We show that the physical parameters associated with nova systems can be estimated by comparing these line ratios with those obtained from observed spectra. We illustrate the idea with examples and estimate the parameter values for a few other novae. The results of the grid model are available online.

Key words: methods: observational – techniques: spectroscopic – novae, cataclysmic variables.

1 INTRODUCTION

It is well known that novae occur in close, interacting binary systems. The primary component is a compact white dwarf (WD), which could be of type CO or ONe, and the secondary component is generally a main-sequence star or late-type giant. Because the system is very close, with an orbital period <16 h, mass transfer occurs from the secondary star on to its companion. As a result, hydrogen-rich matter from the secondary is accreted on to the WD surface via an accretion disc. Over a period of time, the accreted layer on the WD increases in mass, causing the pressure and temperature at the base of the accreted layer to increase gradually. When critical values of the temperature and pressure are reached, thermonuclear burning of hydrogen sets in, which soon builds up to a thermonuclear runaway (TNR) reaction, releasing huge amounts of energy ($\sim 10^{45}$ erg) in a very short period of time. This is commonly known as a nova outburst. The explosion is accompanied by the ejection of matter with velocities of the order of a few hundreds to thousands of kilometres per second in the form of a discrete shell(s), an optically thick wind, or a combination of both. The detailed theory and the development of nova outbursts have been described in a number of articles, for example Bode & Evans (2008), Starrfield, Iliadis & Hix (2008), Warner (1995) and BASI (2012).

Observationally, the outburst is accompanied by a sudden rise in optical brightness, generally with a rise in amplitude of ∼7 to 15 mag in 1 – 2d. The peak luminosities may be as high as 10^4 – 10^5 $L_\odot$ above the quiescence-phase brightness of the object. This is followed by a gradual decrease in the light-curve on time-scales of months to years. All aspects of the outburst are manifested at various stages in the evolution of nova spectra. During the early stage (fireball phase), when the ionization levels are low, the spectrum is generally dominated by permitted, recombination lines of H I, He I, C I, O I, Fe I and N I. As the ejecta expands with time, the density of the ejecta decreases, layers closer to the central ionizing source are revealed, and the degrees of excitation and ionization increase. Forbidden and high-ionization emission lines are seen at this stage. For example, prominent lines of [Fe VI], [Fe VII], [Ca V], [Mn X IV] and [Si VI] are seen in the coronal phase, whereas lines of [Ne III], [O I], [Fe X], [Fe XIV], [Ca XV], [Ni XII] etc. are observed in the nebular phase. As the nova approaches its post-outburst quiescence phase, the ionization levels decrease once again. Thus, the study of the observational properties of emitted spectra may help us to understand the properties of the system.

A number of previous studies attempted to explain observational properties such as light-curves, characteristic times, and the formation of spectrum in novae (e.g. Prialnik & Kovetz 1995; Yaron et al. 2005; Shara et al. 2010; Hachisu & Kato 2006). Hauschildt & Baron (1995) and Hauschildt et al. (1996, 1997) generated synthetic spectra using the PHOENIX code to study the formation of spectral lines in novae. PHOENIX is a stellar atmosphere code that is designed to produce model spectra of stars for different effective temperatures, masses, metallicities, etc. Similarly, CLOUDY (Ferland et al. 2013, 2017) is an astrophysical plasma code that uses a given density and

★ E-mail: anindita12@bose.res.in

an input spectral energy distribution (SED) (e.g. for stars, active galactic nuclei, etc.) to calculate various physical processes and predict the spectrum as the radiation interacts with gas and dust of known composition and geometry under a broad range of conditions. Both codes, CLOUDY and PHOENIX, can be used to simulate 1D and 3D non-local thermodynamic equilibrium models of nova spectra. PHOENIX is basically used as a stellar atmosphere code, whereas the photoionization code CLOUDY has a wider range of applicability, with a larger atomic, molecular and chemical database. Therefore, CLOUDY has the potential to provide better results for nova systems, in which photoionization plays the most important role in generating the emission-line spectra.

In this paper, we calculate simple grid models of novae using the photoionization code CLOUDY (version c17.00 rc1) (Ferland et al. 2017). Our aim is to investigate how the spectral emission-line intensities change under different physical conditions and whether the line ratios can be used to estimate the physical parameters from the observed spectra of novae. In order to do this, we construct a grid of 1792 models for different sets of parameters associated with nova systems, namely the inner radius ($R_{\rm in}$) of the ejected shell, the thickness of the ejected shell (ΔR), the source temperature ($T_{\rm BB}$), the source luminosity (L) and theH density ($n_{\rm H}$) of the ejecta. For each set of parameters, spectra are generated over a wide range of wavelength, from the ultraviolet to the infrared. Next, we calculate the ratios of hydrogen and helium line fluxes (relative to Hβ), which are prominent in nova spectra, and generate a database. We explain how these line ratios can be used to estimate the parameters associated with the system, for example $T_{\rm BB}$, L and $n_{\rm H}$, using information derived from observed spectra. We emphasize here that it is very difficult to obtain information about these parameters directly from observations. Our paper is organized as follows: the modelling procedure is discussed in detail in Section 2, the results are discussed in Section 3, and a summary and the conclusions are given in Section 4.

2 NOVA GRID CALCULATION

As a first step, we constructed the grid model under some basic assumptions. First, we considered dust-free novae. This is because most novae that have been observed do not show evidence of dust formation, and even for the novae that do, the dust does not form for a few weeks, when the temperatures of silicate and graphite grain decrease below their respective sublimation temperatures. Here, however, we are interested primarily in nova characteristics in their early phase, when more observations are available. Second, in order to limit computational time and to set basic abundances, we restricted ourselves to solar metallicity as an average metallicity. It is possible that the model has some limitations, as it is based on simple assumptions, but we show that the method gives reliable estimates of the nova parameters. We are currently working on constructing grid models that incorporate dust and higher metallicities, and these will be presented in a future paper.

We used the photoionization code CLOUDY (version c17.00 rc1) (Ferland et al. 2017) to generate synthetic spectra of several novae. CLOUDY is based on a self-consistent *ab initio* calculation of the thermal, ionization and chemical balance. It uses a minimum number of input parameters and generates output spectra, or vice versa. Previously, CLOUDY has been used to determine the elemental abundances and physical characteristics of a few individual nova, for example LMC 1991 (Schwarz et al. 2001), QU Vul (Schwarz 2002), V1974Cyg (Vanlandingham et al. 2005), V838 Her and V4160 Sgr (Schwarz et al. 2007a), V1186 Sco (Schwarz et al. 2007b), V1065 Cen (Helton et al. 2010) and RS Oph (Mondal et al. 2018, Das & Mondal 2015). Following a similar strategy, we planned to generate a grid of nova models to predict physical parameters constrained by observed hydrogen and helium line intensity ratios. For our nova grid models, we considered a spherically expanding ejecta illuminated by a central WD. We assumed the central source engine to be a blackbody with surface temperature T_{BB} (in K) and luminosity L (in erg s^{-1}). Our calculations included the effects of important ionization (photo, Auger, collisional, charge transfer) and recombination (radiative, dielectronic, three-body recombination, charge transfer) processes.

In addition to this, we assumed that half of the radiation field emitted by the central object actually strikes the gas. The dimensions of the spherical ejecta are defined by the inner and outer radii ($R_{\rm in}$, $R_{\rm out}$), and the density of the ejecta is set by the total hydrogen density given by

$$n(H) = n(H^0) + n(H^+) + 2n(H_2) + \sum_{\rm other} n(H_{\rm other})\,{\rm cm}^{-3},$$

where $n(H_{\rm other})$ represents the H in all other hydrogen-bearing molecules. Following Bath & Shaviv (1976), we assumed a radius-dependent power-law density profile with exponent α, ($n(R) \propto R^{\alpha}$), where $n(R)$ is the density of the ejecta. Starrfield (1989) argued that, for nova photospheres, the value of this exponent can only be -2 or -3. A constant mass-loss rate and a constant velocity for the ejecta gives rise to a value of -2. However, we assumed a constant mass-loss rate together with a velocity proportional to the radius from the source. This gives rise to a value of -3 for the exponent, and we used this value in all our models calculated here:

$$n(R) = n(R_{\rm in}) \left(\frac{R}{R_{\rm in}}\right)^{\alpha}, \qquad \alpha = -3.$$

Here, $n(R_{\rm in})$ is the density at the illuminated face of the cloud at $R_{\rm in}$. In previous calculations by various authors (e.g. Schwarz et al. 1997, 2007b; Helton et al. 2010; Schwarz 2002, etc.), the value of α was also chosen as -3. We considered a clumpy medium with a filling factor 0.1 and varied the inner radius of the ejecta ($R_{\rm in}$), the thickness of the ejecta (ΔR), the temperature of the central source ($T_{\rm BB}$), the luminosity of the central source (L), and the hydrogen density ($n_{\rm H}$). All models were calculated using solar metallicity.

Wide ranges of values for each of these above-mentioned parameters were considered, and the limiting values were chosen on the basis of the available observational results of various classical and recurrent novae in order to construct the grid model. For example, the inner and outer radii were calculated by multiplying the velocities (which can be calculated from the line-widths) by time, and the thickness was calculated by subtracting the inner radius from the outer one. The upper and lower limits of the radii were determined by considering a high velocity of nova ejecta of 10 000 km s^{-1} (e.g. U Sco, Banerjee et al. 2010) and a lower expansion value of 300 km s^{-1} (e.g. V723 Cas, Iijima, 2006). Because emission lines generally start to be resolved about a week after outburst, in the present calculation we considered time from day 5 and calculated up to day 120 after outburst. On the basis of the above values, the limiting values of log($R_{\rm in}$) (in cm) and log(ΔR) (in cm) were chosen as 13.5 and 15.0, with a step-size of 0.5. Similarly, we determined the limiting values of other parameters, namely temperature, luminosity and hydrogen density, on the basis of available observational results. For the temperature ($T_{\rm BB}$) (in K) and luminosity(L) (in erg s^{-1}) of the ionizing source, we considered log($T_{\rm BB}$) $\in$ [4.5, 6.0] with a step-size of 0.5 and log(L) $\in$ [36.0, 39.0] with

Table 1. List of the parameters and the range of their values considered for the grid model.

Parameter	Units	Range	Step-size
Inner radius ($R_{\rm in}$)	cm	$13.5 \leq \log(R_{\rm in}) \leq 15.0$	0.5
Thickness (ΔR)	cm	$13.5 \leq \log(\Delta R) \leq 15.0$	0.5
Temperature ($T_{\rm BB}$)	K	$4.5 \leq \log(T_{\rm BB}) \leq 6.0$	0.5
Luminosity (L)	erg s^{-1}	$36.0 \leq \log(L) \leq 39.0$	1.0
H density ($n_{\rm H}$)	cm^{-3}	$6.0 \leq \log(n_{\rm H}) \leq 12.0$	1.0

a step-size of 1.0. Finally, we took $\log(n_{\rm H})$ (in cm^{-3}) $\in$ [6.0, 12.0] with a step-size of 1.0. Details of the parameter values are presented in Table 1. Our calculations stop at the thickness (ΔR) taken for a particular model. Thus a total of 1792 models were constructed by varying each of these parameters. The results, namely the ratio of line fluxes, are arranged in 256 tables. These 256 tables of the dataset are available at the website https://aninditamondal1001.wixsite.com/researchworks under the button 'NOVAE GRID DATA' on the page *Research/List-of-Documents*. Please acknowledge by citing this paper while using the database. The structure of the tables is shown in Fig. 1.

3 RESULTS

From the model-generated spectra, we calculated the fluxes of 56 hydrogen and helium recombination lines that are generally prominent in nova emission spectra, covering a wide wavelength region. As an example, we present the results of such a model for $\log(R_{\rm in})$ = 15.0 (in cm), $\log(\Delta R)$ = 14.0 (in cm), $\log(T_{\rm BB})$ = 5.5 (in K) and $\log(L)$ = 36 (in erg s^{-1}) in Table 2 (corresponding to table 217 of the database). Line fluxes were calculated for seven values of $\log(n_{\rm H})$ (in cm^{-3}) (i.e. for $n_{\rm H}$ = 10^6, 10^7, 10^8, 10^9, 10^{10}, 10^{11} and 10^{12}). Contours of line flux ratios (along the z-axis) can be plotted against any two parameters (among $T_{\rm BB}$, L and $n_{\rm H}$) along the x- and y-axes, keeping the other one fixed. A typical contour plot of the Hα line flux ratio is shown in Fig. 2, with $\log(L)$ along the x-axis and $\log(n_{\rm H})$ along the y-axis, for $\log(R_{\rm in})$ = 15.0 (in cm), $\log(\Delta R)$ = 14.0 (in cm) and $\log(T_{\rm BB})$ = 5.5 (in K), corresponding to tables 217 – 220 of the database (see Fig. 1 and Table 2). The values of line flux ratios of Hα with respect to (w.r.t.) Hβ are marked on the contours.

As noted above in Section 2, $R_{\rm in}$ and ΔR can be calculated from line-widths and time elapsed since outburst; $T_{\rm BB}$ can be obtained by blackbody fitting with the continuum of the observed spectra; and line fluxes can be measured from the observed spectra. Once the values of $R_{\rm in}$, ΔR and $T_{\rm BB}$ are found, we can choose the corresponding dataset from the database and make contour plots for different lines, for example Hα, Hγ, Hδ. From these contour plots we can extract (e.g. Fig. 2) the contours for the corresponding values of the line ratios and plot them together (e.g. Fig. 3). From the intersection of the contours of different lines, we can determine the values of the parameters, namely L and $n_{\rm H}$ (in the case of Fig. 3). In this way, by knowing the value of any one of L, $n_{\rm H}$ and $T_{\rm BB}$, the values of the other two can be determined.

To check if this method works well, we applied this method to a number of novae. First, we consider RS Ophiuchi (RS Oph), which is a well-known recurrent nova (recurrence period ~20 yr). From the optical spectra taken 12 d after outburst (2006) with the 2-m Himalayan Chandra Telescope (HCT), we calculated the temperature as $10^{4.5}$ K and the line flux ratios of Hα, Hγ, Hδ and Hε w.r.t. Hβ as 6.12, 0.39, 0.28 and 0.29, respectively (Mondal et al. 2018). From the expansion velocities of the ejecta (see section 5 in Mondal et al. 2018), we calculated $R_{\rm in}$ and ΔR. For this particular set of $R_{\rm in}$, ΔR and $T_{\rm BB}$, we plotted contours for the hydrogen lines with L and $n_{\rm H}$ along the x- and y-axis. We extracted the contours for the corresponding values of the line ratios and plotted them together (Fig. 3). From the figure, we find that all lines intersect at $\log(L)$ = 36.65 (in erg s^{-1}) and $\log(n_{\rm H})$ = 10.2 (in cm^{-3}). These values are consistent with previous results for RS Oph (see Table 3).

We also ran a separate CLOUDY model for RS Oph considering the derived parameter values and generated a synthetic spectrum,keeping the abundances as solar. The simulated spectrum was then compared with the observed one taken with the 2-m HCT in the optical region. In Fig. 4, the observed spectrum is shown with a solid black line, and the simulated spectrum is shown with a dashed red line. It is clearly seen that the observed hydrogen features match the modelled hydrogen lines well. This, alternatively, validate our method of estimating parameters.

In a similar way, we also tested our grid model for other galactic classical novae, for example for V1065 Cen, V1186 Sco, V1974 Cyg and PW Vul, to determine the physical parameters. For novae RS Oph, V1065 Cen and V1974 Cyg, we could estimate the parameter values using only hydrogen lines. For novae V1186 Sco and PW Vul, however, the contours of the hydrogen lines (optical, near-infrared and far-infrared) intersected at multiple points. We therefore used the He I 1.083 μm line (for V1186 Sco) and the He II 4686 Å line (for PW Vul), which are strong in the spectra, along with other hydrogen lines to estimate the parameters. It should be noted here that, from previous studies, we found the He abundances w.r.t. solar as 1.1 ± 0.3 in the case of V1186 Sco (Schwarz et al. 2007b) and as 1.0 ± 0.4 in the case of PW Vul (Schwarz et al. 1997), which are near to solar values. So, there are no significant changes in the intensities of He lines, and it is reasonable to use these linesto estimate the parameters. Our results, which are shown in Table 3, match well with the previously calculated results. These results validated the method and motivated us to apply it to a few other novae and to estimate the values of the physical parameters.

(i) **Nova KT Eridin (KT Eri)**: this is a well-known galactic classical nova, discovered by K. Itagaki on 2009 November 25.5 UT (Yamaoka et al. 2009). The maximum and minimum velocities of the ejecta were determined as $V_{\rm max}$ = 3600 km s^{-1}, $V_{\rm min}$ = 1900 km s^{-1}, respectively, from the broad Balmer emission features (Maehara, Arai & Isogai 2009). From the SMARTS (Small & Moderate Aperture Research Telescope System) spectroscopic data (Walter et al. 2012), taken 12 d after outburst, we calculated $T_{\rm BB}$ = 10^5 K. The line flux ratio of Hα and Hγ w.r.t. Hβ were measured as 2.87 and 0.78, respectively. Using the values in the database, we plotted the contours for the hydrogen lines for the particular set of $R_{\rm in}$, ΔR and $T_{\rm BB}$. We then extracted contours for the observed line fluxes together (Fig. 5), and from the intersection of the lines we estimated $\log(L)$ = 38.5 (in erg s^{-1}) and $\log(n_{\rm H})$ = 9.2 (in cm^{-3}).

(ii) **V5558 Sagittarii (V5558 Sgr)**: this nova was discovered on 2007 April 14.77 UT. The values of $R_{\rm in}$ and ΔR on 24 d after outburst were calculated using the minimum ($V_{\rm min}$ = 250 km s^{-1}) and maximum ($V_{\rm max}$ = 540 km s^{-1}) expansion velocities of the ejecta (Iijima 2007a, b). From the continuum of the optical spectra, we measured the temperature to be 10^6 K. We calculated the line flux ratios of Hγ and Hδ w.r.t. Hβ and of Paβ w.r.t. Paγ from the spectra taken in the optical (Tanaka et al. 2011) and the near-infrared region (Das et al. 2015), respectively. Next we plotted the corresponding contours from the database. We then extracted the contours for the

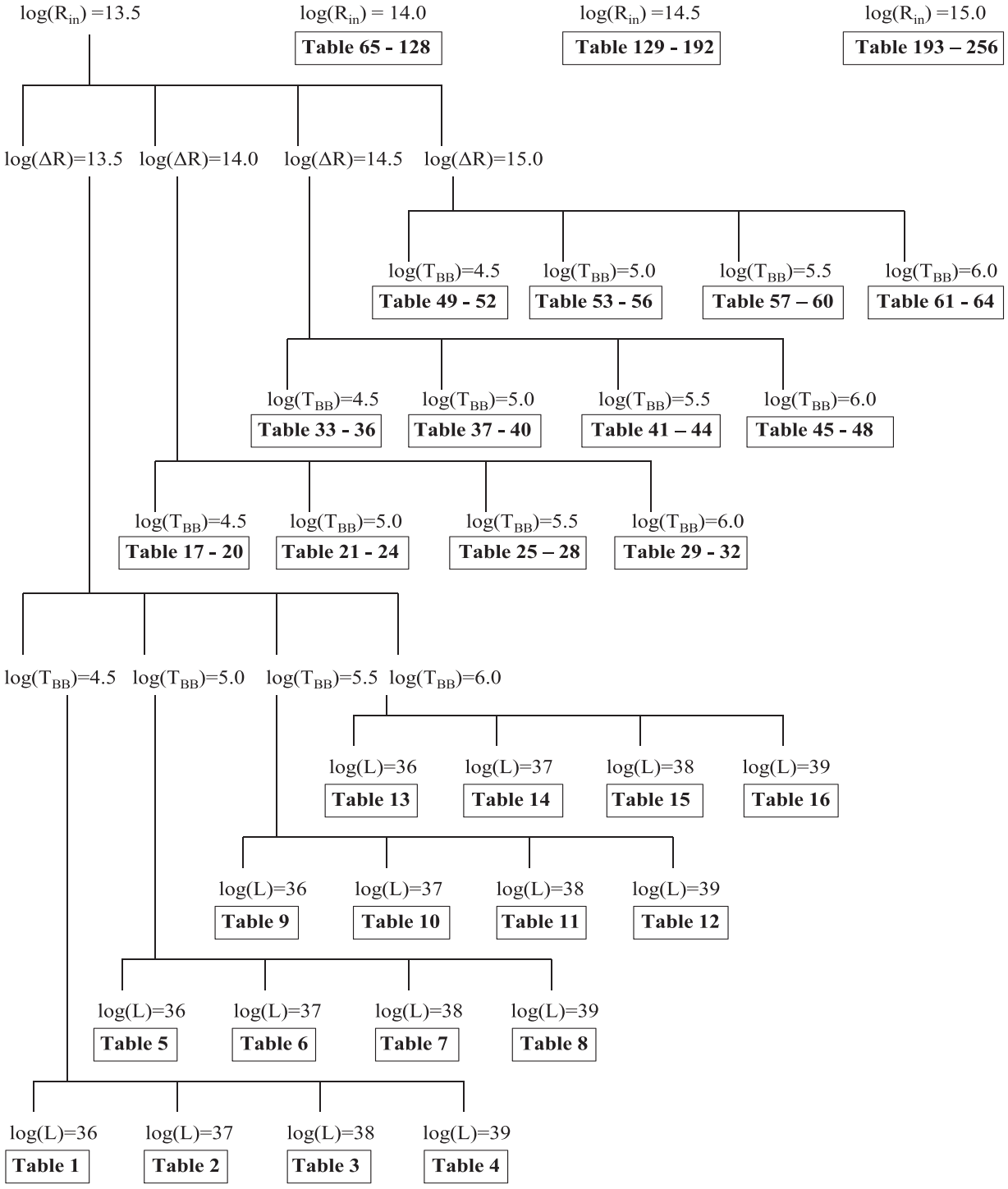

Figure 1. Schematic diagram of the structure of datasets of nova grid models. Each table contains data for $\log(n_{\rm H}) = 6$–12 [in cm^{-3}] with a step-size of 1. See Sections 2 and 3 for details.

observed line ratios and plotted them together (Fig. 6). From the intersection of the extracted contours for the observed line ratios, we estimated $L = 6.4 \times 10^{38}$ erg s^{-1} and $n_{\rm H} = 3.4 \times 10^{9}$ cm^{-3}. This example shows that lines in other wavelength regions may sometimes help to determine the values more precisely. A more detailed study of this nova using CLOUDY is in progress and will be presented in a future paper.

(iii) **U Scorpii (U Sco)**: the recurrent nova U Sco explodes at intervals of 10 ± 2 yr, with the most recent outburst having occurred on 2010 January 28 (Schaefer et al. 2010). From the optical spectra taken about 6 d after outburst, the maximum velocity was calculated from the He I 7065 Å line as ∼ 9900 km s^{-1}, whereas the minimum velocity was calculated as ∼ 3786 km s^{-1} from the hydrogen lines (Anupama et al. 2013). During the early phase, the

Table 2. Normalized fluxes of hydrogen and helium emission lines w.r.t. Hβ for log($R_{\rm in}$) = 15.0 (in cm), log(ΔR) = 14.0 (in cm), log($T_{\rm BB}$) = 5.5 (in K), log(L) = 36 (in erg s^{-1}), with log($n_{\rm H}$) = 6–12 (in cm^{-3}) with a step-size of 1, corresponding to table 217 of the database (see Fig. 1).

Line ID	Wavelength	log(n_H) [cm^{-3}]						
	λ (μm)	6	7	8	9	10	11	12
Ly C	0.0912	2.9190E+01	3.8110E+00	1.1920E-04	0.0000E+00	0.0000E+00	0.0000E+00	1.0110E-12
Ly 6	0.0938	4.2240E-01	1.0540E-02	8.6260E-04	8.2940E-04	9.0570E-04	9.0190E-04	9.8810E-04
Ly δ	0.0950	5.8950E-01	1.2230E-02	1.0530E-03	9.0530E-04	9.2350E-04	8.0760E-04	8.3480E-04
Ly γ	0.0973	7.2740E-01	1.2930E-02	1.6130E-03	1.2480E-03	1.1170E-03	8.8430E-04	7.7610E-04
Ly β	0.1026	1.0550E+00	1.7060E-02	3.5310E-03	3.0670E-03	2.5570E-03	1.8120E-03	1.3320E-03
Ly α	0.1216	6.7540E+01	6.1440E+01	1.1850E+02	1.2060E+02	1.0100E+02	7.6470E+01	5.3090E+01
H C	0.3646	1.6910E+00	1.4870E+00	1.3630E+00	1.3360E+00	1.2080E+00	9.4060E-01	6.7300E-01
H 7	0.3970	1.4510E-01	1.6930E-01	2.0370E-01	2.3040E-01	2.5220E-01	2.3080E-01	2.8630E-01
H δ	0.4102	2.4260E-01	2.6100E-01	3.0420E-01	3.3240E-01	3.5400E-01	3.8010E-01	4.0200E-01
H γ	0.4340	4.5850E-01	4.6670E-01	4.9190E-01	5.1650E-01	5.3250E-01	5.5070E-01	5.7270E-01
He I	0.4388	3.2860E-05	3.8380E-04	6.3160E-03	1.2510E-02	1.7170E-02	1.7270E-02	1.3040E-02
He I	0.4471	3.1270E-04	3.3640E-03	5.0270E-02	9.4240E-02	1.1710E-01	1.0480E-01	7.2410E-02
He II	0.4686	6.8820E-01	6.7630E-01	3.7720E-01	1.7450E-01	5.6540E-02	1.3110E-02	2.0670E-03
H β	0.4861	1.0000E+00	1.0000E+00	1.0000E+00	1.0000E+00	1.0000E+00	1.0000E+00	1.0000E+00
He I	0.5016	1.2640E-05	6.6130E-04	3.1700E-02	6.1880E-02	7.8150E-02	7.0440E-02	4.9750E-02
H α	0.6563	3.0620E+00	2.9570E+00	4.1380E+00	4.9410E+00	5.5690E+00	5.8580E+00	5.8720E+00
He I	0.6678	2.3330E-04	2.6540E-03	4.1060E-02	7.8710E-02	9.7380E-02	8.4280E-02	5.5030E-02
He I	0.7065	5.3470E-04	5.5940E-03	6.7980E-02	1.2850E-01	1.3610E-01	9.7780E-02	4.9230E-02
Pa C	0.8204	3.5220E-01	2.9580E-01	2.5590E-01	2.4380E-01	2.1670E-01	1.6840E-01	1.2060E-01
Pa 9	0.9229	2.3490E-02	2.6460E-02	3.5670E-02	4.5440E-02	5.4750E-02	5.7910E-02	5.6870E-02
Pa 8	0.9546	3.2700E-02	3.6490E-02	4.7920E-02	5.8920E-02	7.0910E-02	7.7140E-02	7.7890E-02
Pa δ	1.0049	4.8790E-02	5.3080E-02	6.9660E-02	8.2540E-02	9.6060E-02	1.0620E-01	1.0710E-01
He I	1.0830	1.5530E-02	1.7610E-01	1.9340E+00	4.5530E+00	6.1130E+00	5.4110E+00	3.3060E+00
Pa γ	1.0938	8.1120E-02	8.3250E-02	1.1070E-01	1.2920E-01	1.4340E-01	1.4940E-01	1.5040E-01
He II	1.1627	3.4190E-02	3.3190E-02	1.5790E-02	7.1870E-03	2.4220E-03	5.9830E-04	1.0090E-04
He I	1.1969	1.3500E-05	1.5040E-04	2.3670E-03	4.5540E-03	6.0650E-03	6.1390E-03	5.0290E-03
He I	1.2527	1.1200E-05	1.2490E-04	2.3650E-03	4.1690E-03	4.1850E-03	2.9790E-03	1.6330E-03
Pa β	1.2818	1.3940E-01	1.4170E-01	1.9280E-01	2.2880E-01	2.5230E-01	2.5150E-01	2.4210E-01
Br 20	1.5192	1.4960E-03	2.1150E-03	3.4490E-03	4.5010E-03	4.9900E-03	4.7170E-03	3.7980E-03
Br 19	1.5260	1.7180E-03	2.3770E-03	3.9180E-03	5.1640E-03	5.7750E-03	5.4910E-03	4.4410E-03
Br 18	1.5342	1.9930E-03	2.6890E-03	4.4630E-03	5.9460E-03	6.7180E-03	6.4340E-03	5.2330E-03
Br 17	1.5439	2.3350E-03	3.0680E-03	5.0950E-03	6.8670E-03	7.8520E-03	7.5870E-03	6.2150E-03
Br 16	1.5556	2.7680E-03	3.5450E-03	5.8320E-03	7.9500E-03	9.2170E-03	9.0030E-03	7.4390E-03
Br 15	1.5701	3.3260E-03	4.1590E-03	6.7000E-03	9.2230E-03	1.0860E-02	1.0740E-02	8.9730E-03
Br 14	1.5880	4.0580E-03	4.9650E-03	7.7390E-03	1.0730E-02	1.2830E-02	1.2890E-02	1.0890E-02
Br 13	1.6109	5.0410E-03	6.0400E-03	9.0360E-03	1.2540E-02	1.5190E-02	1.5520E-02	1.3280E-02
Br 12	1.6407	6.3920E-03	7.5050E-03	1.0760E-02	1.4790E-02	1.8010E-02	1.8700E-02	1.6190E-02
Br 11	1.6806	8.3030E-03	9.5620E-03	1.3180E-02	1.7700E-02	2.1390E-02	2.2520E-02	1.9680E-02
He I	1.7003	2.2110E-05	2.3790E-04	3.5560E-03	6.6670E-03	8.2830E-03	7.4150E-03	5.3760E-03
Br 10	1.7362	7.6950E-03	8.7790E-03	1.2330E-02	1.5620E-02	1.8300E-02	1.8710E-02	1.8320E-02
Br 9	1.8174	1.0450E-02	1.1330E-02	1.5200E-02	1.9340E-02	2.3300E-02	2.4640E-02	2.4920E-02
Pa α	1.8751	2.8440E-01	2.7860E-01	4.1780E-01	5.1640E-01	5.7850E-01	5.7250E-01	5.3670E-01
Br δ	1.9446	1.4910E-02	1.5680E-02	2.0380E-02	2.4990E-02	3.0050E-02	3.2680E-02	3.3900E-02
He I	2.0581	7.0750E-07	1.7650E-04	4.1300E-02	1.2850E-01	2.3440E-01	2.6670E-01	1.9320E-01
He I	2.1130	2.7780E-06	2.9060E-05	3.8350E-04	6.8760E-04	7.6670E-04	5.8670E-04	3.4470E-04
Br γ	2.1655	2.2750E-02	2.3090E-02	2.9590E-02	3.4830E-02	4.0430E-02	4.4670E-02	4.6070E-02
Br β	2.6252	3.8300E-02	3.6890E-02	4.6910E-02	5.3890E-02	5.9490E-02	6.1790E-02	6.3500E-02
Pf 10	3.0384	4.0130E-03	4.5100E-03	6.3250E-03	8.0140E-03	9.3860E-03	9.5950E-03	9.3460E-03
Pf 9	3.2961	5.5080E-03	5.8080E-03	7.7740E-03	9.8810E-03	1.1900E-02	1.2580E-02	1.2640E-02
Pf γ	3.7400	7.9990E-03	8.0270E-03	1.0360E-02	1.2680E-02	1.5240E-02	1.6560E-02	1.7150E-02
Br α	4.0512	6.3160E-02	5.9880E-02	7.7720E-02	9.0410E-02	9.8890E-02	9.8270E-02	9.6580E-02
Pf β	4.6525	1.2430E-02	1.1780E-02	1.4840E-02	1.7390E-02	2.0160E-02	2.2250E-02	2.3070E-02
Hu γ	5.9066	3.2200E-03	3.3250E-03	4.4410E-03	5.6420E-03	6.7920E-03	7.1820E-03	7.2460E-03
Pf α	7.4578	2.1030E-02	1.8280E-02	2.2390E-02	2.5420E-02	2.7950E-02	2.8990E-02	3.0160E-02
Hu β	7.5004	4.7050E-03	4.5330E-03	5.8230E-03	7.1170E-03	8.5480E-03	9.2910E-03	9.6840E-03
Hu α	12.3685	7.2340E-03	6.3200E-03	7.8650E-03	9.1900E-03	1.0640E-02	1.1740E-02	1.2300E-02

effective temperature was measured as 2×10^4 K and the electron density as $10^{7.8}$ cm^{-3} (Anupama et al. 2013). Line fluxes of Hα, Hγ and Hδ w.r.t. Hβ were measured as 2.45, 0.72 and 0.38. Then, following a similar method, from the extracted contour plots (Fig. 7) we estimated $n_{\rm H} = 10^8$ cm^{-3} and $L = 10^{37.8}$ erg s^{-1}, which match the previously obtained results well (see Table 4).

(iv) **V339 Delphini (V339 Del)**: on 14.584 August 2013, Koichi Itagaki discovered the classical nova Delphini 2013 (V339 Del)

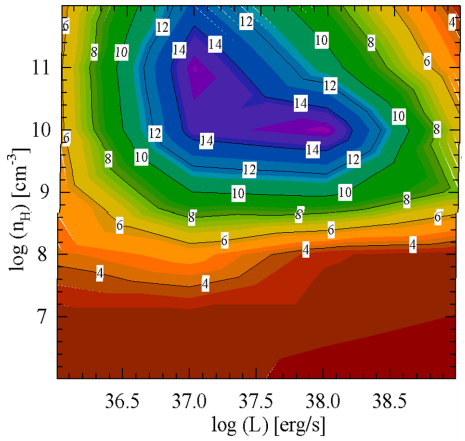

Figure 2. Contour plot of the Hα line flux ratio w.r.t. Hβ for log(R_{in}) = 15.0 (in cm), log(ΔR) = 14.0 (in cm) and log(T_{BB}) = 5.5 (in K); log(L) (in erg s^{-1}) and log(n_H) (in cm^{-3}) are plotted along the x- and y-axis respectively, corresponding to tables 217–220 of the database (see Fig. 1). The values of Hα/Hβ are marked on each contour. See Section 3 for further details.

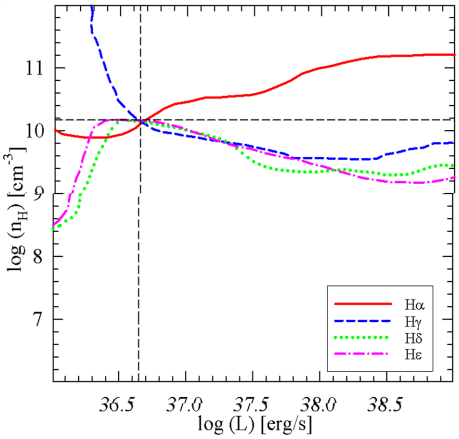

Figure 3. Plots of various extracted contour lines for nova RS Oph, 12 d after outburst. The red solid, blue short-dashed, green dotted, and pink dot–dashed lines represent the extracted plots of line flux ratios of Hα, Hγ, Hδ and Hε respectively w.r.t. Hβ. The lines intersect at log(L) = 36.65 (in erg s^{-1}) and log(n_H) = 10.2 (in cm^{-3}). See Section 3 for further details.

at an optical magnitude of 6.8 (Nakamo et al. 2013). Burlak et al. (2015) calculated the luminosity of the system as $10^{38.39}$ erg s^{-1} from the early-phase spectrum, and the expansion velocity was calculated to be in the range 1000–1800 km s^{-1} from the Hα emission lines. We measured the Balmer line flux ratios from the spectra taken 21 d after the outburst as Hα/Hβ = 6.34 and Hγ/Hβ = 0.34. Fig. 8 shows the contour plots of the hydrogen line flux ratios, with T_{BB} and n_H along the x- and y-axis, respectively. The lines intersect at log(T_{BB}) = 5.51 (in K) and log(n_H) = 9.78 (in cm^{-3}), which give the values of T_{BB} and n_H, respectively.

(v) **IC 1613 #2015**: this is an extragalactic classical nova in the dwarf galaxy IC 1613 discovered on 2015 September 10. The values of V_{max} and V_{min} were calculated from the Hα emission line and Hγ absorption line as ∼1750 and 1200 km s^{-1}, respectively (Williams, Darnley & Henze 2017). From *Swift* X-rays studies, the temperature and luminosity of the source were determined to be $T_{BB} = 10^{5.76}$ K and $L = 10^{37.7}$ erg s^{-1} (Williams et al. 2017). We used the line flux ratios of Hα, Hγ and Hδ w.r.t. Hβ measured 26 d after outburst to find the values of other observables. The extracted contours of the line flux ratios from the grid database give log(L) = 37.9 (in erg s^{-1}), which matches well with $L = 10^{37.7}$ erg s^{-1} from the X-ray study, and log(n_H) = 11.7 (in cm^{-3}). The plot is shown in Fig. 9, and the parameter values are shown in Table 4 in more detail.

4 SUMMARY AND DISCUSSION

We have computed grid models of novae using the photoionization code CLOUDY (Ferland et al. 2017). The aim of this paper has been to generate an extended 5D parameter space for dust-free novae by varying the hydrogen density, the inner radius and thickness of the nova ejecta, and the temperature and the luminosity of the ionizing source commensurate with observed ranges. From the model-generated synthetic spectra we calculated line intensities of 56 hydrogen and helium lines, which are generally observed prominently in nova spectra, spanning over a wide range of wavelengths: from the ultraviolet to the infrared.

The simulated hydrogen and helium line intensities of our grid can be compared with observations, and physical parameters such as T_{BB}, L and n_H can be inferred. To test the robustness of our calculations, we cross-checked predictions from our grid results for a few novae, namely RS Oph, V1065 Cen, V1974 Cyg, V1186 Sco and PW Vul, with published data and found that they matched well. We also estimated the density, luminosity and temperature of five other novae, one of which is an extragalactic nova. We have demonstrated that our grid models work well. This gives us confidence that this methodwill work successfully. However, there is scope to improve the models, as discussed below.

We considered dust-free environments, because observations show that most novae do not form dust. Measurements of the fluxes of spectral lines in the post-dust-formation phase may not yield accurate results. Caution should therefore be exercised when measuring the line fluxes. We plan to incorporate dust in our model and to determine the effect of dust on the line intensities in the future. In addition, in the present calculations we used solar abundances in order to limit the computational time. If the abundances of elements other than hydrogen are increased or decreased, the hydrogen line intensities may change. To investigate this, we constructed a few models with higher metallicity (2, 2.5 and 3 times solar metallicity) and found that variations in hydrogen line intensities are less than 15%. We are in the process of extending our database with results for different metallicities.

In the present calculation, we have not incorporated errors associated with the measurements of the values of observables, in order to keep our model simple. To check how the errors affect the results, we considered a ±5 per cent error associated with observed line fluxes for nova V5558 Sgr. The results are shown on a linear scale in Fig. 10. We also checked on a log scale that the curves do not intersect at any other points, even after inclusion of the error margins. From Fig. 10, we find the modified results to be $L = (6.1 - 6.8) \times 10^{38}$ erg s^{-1} and $n_H = (3.2 - 3.4) \times 10^9$ cm^{-3}. These are in agreement with the previous results of $L = (6.4 \pm 0.4) \times 10^{38}$ erg s^{-1} and $n_H = (3.3 \pm 0.1) \times 10^9$ cm^{-3}. Thus the uncertainties are lower (∼ 6.25 % in the case of L and ∼ 5.8 % in the case of n_H), which ensures the applicability of the method. If uncertainties in the observables increase, the results will likewise become more uncertain. So, caution should be exercised when choosing the emission lines. It is suggested that strong emission lines (e.g. Hα, Hβ, Hγ, Paα, Paβ, Paγ, Brγ etc.) should be considered in order to reduce the error during measurements.

The nature of the contours depends on the line ratios, and the line intensity varies from nova to nova. In a few cases, degeneracy may

Table 3. Comparison of estimated parameter values for various novae obtained from the grid model with previously calculated results (shown in parentheses).

Nova (Outburst)	Line flux ratio from literature	Ref.	Estimated values (previously calculated values)				
			log(R_{in}) [cm]	log(ΔR) [cm]	log(T_{BB}) [K]	log(L) [erg s^{-1}]	log(n_H) [cm^{-3}]
RS Oph (2006)	Hα/Hβ = 6.12, Hγ/Hβ = 0.39, Hδ/Hβ = 0.28, Hε/Hβ = 0.29	1	14.0 (14.0[1])	14.0 (14.05[1])	4.5 (4.5[1])	36.65 (36.8[1])	10.2 (10.5[1])
V1065 Cen (2007)	Hα/Hβ = 3.89, Hγ/Hβ = 0.48, Paγ/Paβ = 0.61	2	15.0 (15.16[2])	15.0 (15.02[2])	5.0 (4.77[2])	38.0 (38.05[2])	7.5 (7.52[2])
V1186 Sco (2004)	Hγ/Hβ = 0.38, Hδ/Hβ = 0.24, Paγ/Paβ = 0.57, Huγ/Huα = 0.65, He I (1.083 μm)/Paβ = 12.14	3	15.0 (15.04[3])	15.0 (15.15[3])	4.5 (4.7[3])	36.8 (36.8[3])	7.5 (7.5[3])
V1974 Cyg (1992)	Hα/Hβ = 2.93, Hγ/Hβ = 0.42	4	15.0 (15.3[4])	15.0 (15.4[4])	5.5 (5.52[4])	38.0 (38.06[4])	8.0 (7.8[4])
PW Vul (1984)	Hα/Hβ = 4.4, Hγ/Hβ = 0.37, He II (4686 Å)/Hβ = 0.34	5	15.0 (15.25[5])	15.0 (15.5[5])	5.5 (5.4[5])	37.7 (37.8[5])	7.1 (7.04[5])

Note. [1]Mondal et al. (2018), Das & Mondal (2015); [2]Helton et al. (2010); [3]Schwarz et al. (2007b); [4]Vanlandingham et al. (2005); [5]Schwarz et al. (1997).

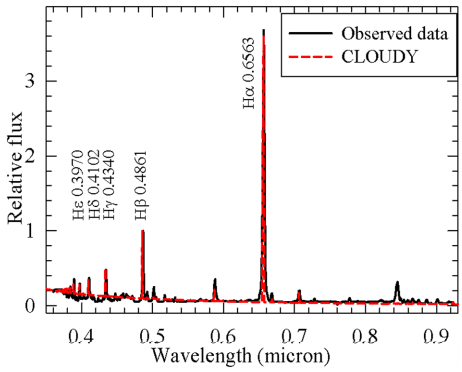

Figure 4. Comparison of observed (solid black) and CLOUDY-generated (dashed red) spectra of nova RS Oph. Prominent hydrogen features are marked. See Section 3 for further details.

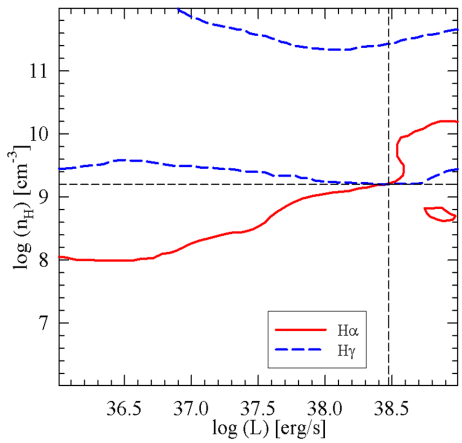

Figure 5. Plots of various extracted contour lines of nova KT Eri, 12 d after outburst. The red solid and blue dashed lines represent the extracted plots of line flux ratios of Hα and Hγ respectively w.r.t. Hβ. The lines intersect at log(L) = 38.5 (in erg s^{-1}) and log(n_H) = 9.2 (in cm^{-3}). See Section 3 for further details.

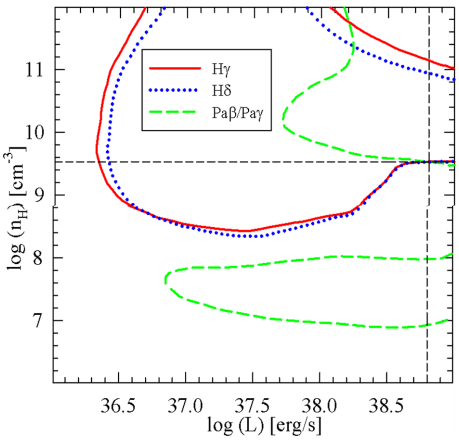

Figure 6. Plots of various extracted contour lines of nova V5558 Sgr, 24 d after outburst. The red solid and blue dotted lines represent the extracted plots of the line flux ratios of Hγ and Hδ respectively w.r.t. Hβ, and the green dashed line represents the extracted plots of line flux ratios of Paβ w.r.t. Paγ. The lines intersect at log(L) = 38.8 (in erg s^{-1}) and log(n_H) = 9.5 (in cm^{-3}). See Section 3 for further details.

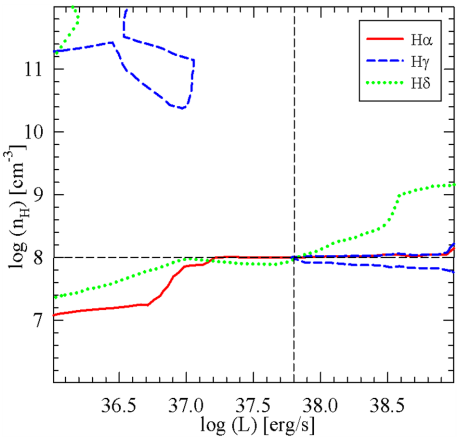

Figure 7. Plots of various extracted contour lines of nova U Sco, 5.81 d after outburst. The red solid, blue short-dashed, and green dotted lines represent the extracted plots of line flux ratios of Hα, Hγ and Hδ respectively w.r.t. Hβ. The lines intersect at log(L) = 37.8 (in erg s^{-1}) and log(n_H) = 8.0 (in cm^{-3}). See Section 3 for further details.

Table 4. Estimated parameter values of selected novae obtained through the CLOUDY grid model.

Nova	Outburst	Line flux ratios	Reference	log(R_{in}) [cm]	log(ΔR) [cm]	log(T_{BB}) [K]	log(L) [erg s^{-1}]	log(n_H) [cm^{-3}]
KT Eri	2009	Hα/Hβ = 2.87, Hγ/Hβ = 0.78	1	14.0	14.0	5.0	38.5	9.2
V5558 Sgr	2007	Hγ/Hβ = 0.52, Hδ/Hβ = 0.20, Paβ/Paγ = 1.14	2	14.5	14.5	6.0	38.8	9.53
U Sco	2010	Hα/Hβ = 2.45, Hγ/Hβ = 0.72, Hδ/Hβ = 0.38	3	14.5	14.5	4.5	37.8	8.0
V339 Del	2013	Hα/Hβ = 6.34, Hγ/Hβ = 0.34	4	14.5	14.0	5.51	38.0	9.78
Nova IC1613 2015	2015	Hα/Hβ = 7.47, Hγ/Hβ = 0.40, Hδ/Hβ = 0.35	5	14.5	14.0	6.0	37.9	11.7

[1]Walter et al. (2012); [2]Tanaka et al. (2011), Das et al. (2015); [3]Anupama et al. (2013); [4]Gherase et al. (2015), Burlak et al. (2015); [5]Williams et al. (2017).

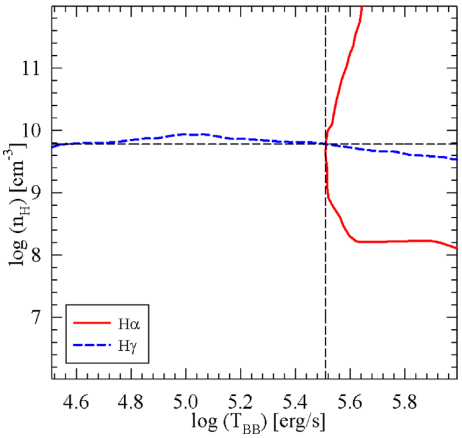

Figure 8. Contour plot of the extracted contour lines of nova V339 Del, 21 d after outburst. The red solid and blue dashed lines represent the contour plots of line flux ratios of Hα and Hγ respectively w.r.t. Hβ. The lines intersect at log(T_{BB}) = 5.51 (in K) and log(n_H) = 9.78 (in cm^{-3}). See Section 3 for further details.

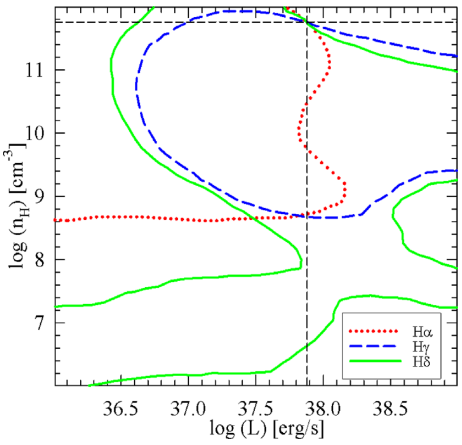

Figure 9. Plots of extracted contour lines of nova 2015 in dwarf galaxy IC1613, 26 d after ouburst. The red dotted, blue dashed and green solid lines represent the extracted plots of the line flux ratios of Hα, Hγ and Hδ respectively w.r.t. Hβ. The results are log(L) = 37.9 (in erg s^{-1}) and log(n_H) = 8.7 (in cm^{-3}). See Section 3 for further details.

appear; that is, more than one contour may follow the same locus or have multiple intersections. For example, in Fig. 6 the curves nearly intersect around log(L) = 38.2 [in erg s^{-1}] and log(n_H) = 11.5 [in cm^{-3}], in addition to the intersection at log(L) = 38.8 [in erg s^{-1}] and log(n_H) = 9.5 [in cm^{-3}]. In such cases, results obtained

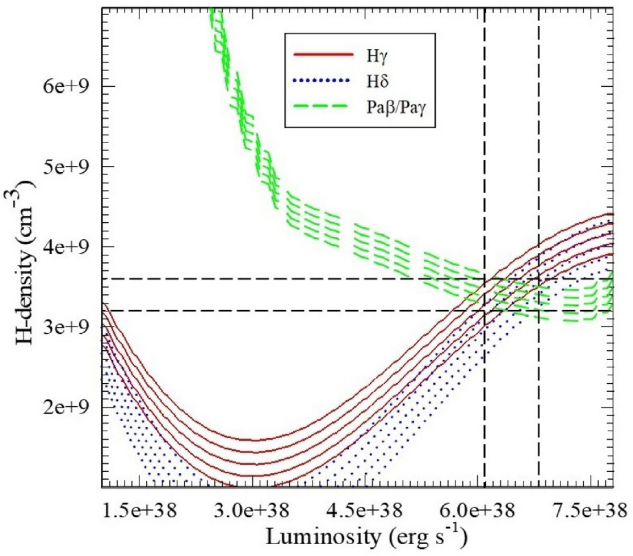

Figure 10. Plot of various extracted contour lines of nova V5558 Sgr, 24 d after outburst, incorporating a 5 per cent error for observed flux values. The red solid and blue dotted lines represent the extracted plots of line flux ratios of Hγ and Hδ respectively w.r.t. Hβ, and the green dashed line represents the extracted plots of line flux ratios of Paβ w.r.t. Paγ. The lines intersect between $L = (6.1- 6.8)\times 10^{38}$ erg s^{-1} and $n_H = (3.2- 3.4)\times 10^{9}$ cm^{-3}. See Section 4 for further details.

from other calculations may help to estimate the parameter values. Furthermore, the use of additional emission lines/observables may ensure that we do not obtain any other intersections. We suggest considering strong emission lines (Hα, Hβ, Hγ, Paα, Paβ, Paγ, Brγ etc.) with higher flux ratios, as they involve lower instrumentation errors during measurements. Generally, the degeneracy does not increase when considering more observables. If it does, we should consider emission lines of other elements (e.g. the He line for nova V1186 Sco) as well.

If we take the line ratios w.r.t. other lines instead of Hβ, the shapes of the contours will be different and degeneracy may not occur. From the plots, strong lines such as the lower members of the hydrogen series have a lower tendency to be degenerate. Multiwavelength observations would therefore be useful in such cases. If there are multiple intersections, results obtained from other calculations may help in estimating the parameter values. We should use as many emission lines/observables as available to make sure that multiple intersections do not occur. If no intersection is found, a range of the values could be estimated.

All of our models presented here are 1D, and radiation from the central source has been approximated as blackbody radiation. It would be interesting to study how more advanced stellar atmospheres, instead of simple blackbody radiation, could affect the results. In the future, we would like to include wind in our models and extend it to three dimensions using an advanced version of pyCLOUDY. Furthermore, a finer mesh could be utilized to determine more precise values of the physical parameters. In addition to optical and infrared spectra, X-ray spectra have been observed in many novae (e.g. V2491 Cyg, Ness et al. 2011; V4743 Sgr, Ness et al. 2003 etc.), and similar grid models could be computed for X-ray spectra. CLOUDY could be used to model all these lines.

For the benefit of the astronomical community, we have kept the database online at https://aninditamondal1001.wixsite.com/researchworks under 'NOVAE GRID DATA' on the page *Research/List-of-Documents*. In addition, a 'Read Me' file is available that describes the structure of the data files. Data can be obtained individually in *.xls format (16.4 KB each). The whole grid (256 tables) has a total size of 4.1 MB.

ACKNOWLEDGEMENTS

The research work at the S. N. Bose National Centre for Basic Sciences is funded by the Department of Science and Technology, Government of India. GS would like to acknowledge the Department of Science and Technology, Government of India, for her WOS-A project SR/WOS-A/PM-9/2017. The authors also thank the anonymous referee for valuable comments and suggestions that helped to improve the quality of the manuscript.

REFERENCES

Anupama G. C. et al., 2013, A&A, 559, A121
Banerjee D. P. K. et al., 2010, MNRAS, 408, L71
Bath G. T., Shaviv G., 1976, MNRAS, 175, 305
Bode M. F., Evans A., eds, 2008, Classical Novae. Cambridge Univ. Press, Cambridge
Bull. Astron. Soc. India, 2012, Special Issue on Classical Novae. Cambridge Univ. Press, Cambridge
Burlak M. A., Esipov V. F., Komissarova G. V., Shenavrin V. I., Taranova O. G., Tatarnikov A. M., Tatarnikova A. A., 2015, Baltic Astron., 24, 109
Das R. K., Mondal A., 2015, New Astron., 39, 19
Das R. K., Banerjee D. P. K., Nandi A., Ashok N. M., Mondal S., 2015, MNRAS, 447, 806
Ferland G. J. et al., 2013, RMxAA, 49, 137
Ferland G. J. et al., 2017, RMxAA, 53, 385
Gherase R. M., Sonka A. B., Popescu M., Naiman M., Micu F., 2015, RoAJ, 25, 241
Hachisu I., Kato M., 2006, ApJS, 167, 59
Hauschildt P. H., Baron E., 1995, J. Quant. Spectrosc. Radiat. Transfer, 54, 987
Hauschildt P. H., Baron E., Starrfield S., Allard F., 1996, ApJ, 462, 386
Hauschildt P. H., Shore S. N., Schwarz G. J., Baron E., Starrfield S., Allard F., 1997, ApJ, 490, 803
Helton L. A. et al., 2010, ApJ, 140, 1347
Iijima T., 2006, A&A, 451, 563
Iijima T., 2007a, Cent. Bur. Elect. Teleg., 934
Iijima T., Correia A. P., Hornoch K., Carvajal J., 2007b, Cent. Bur. Elect. Teleg., 1006
Maehara H., Arai A., Isogai M., 2009, Cent. Bur. Elect. Teleg., 2055, 1
Mondal A., Anupama G. C., Kamath U. S., Das R. K., Selvakumar G., Mondal S., 2018, MNRAS, 474, 4211
Nakamo S. et al., 2013, Cent. Bur. Elect. Teleg., **3628** , edited by Green D. W. E.
Ness J. U. et al., 2003, ApJ, 594, L127
Ness J. U. et al., 2011, ApJ, 733, 70
Prialnik D., Kovetz A., 1995, ApJ, 445, 789P
Schaefer B. E., Harris B. G., Dvorak S., Templeton M., Linnolt M., 2010, IAU Circ., 9111, 1
Schwarz G. J., 2002, ApJ, 577, 940
Schwarz G. J., Starrfield S., Shore S. N., Hauschildt P. H., 1997, MNRAS, 290, 75
Schwarz G. J. et al., 2001, MNRAS, 320, 103
Schwarz G. J. et al., 2007a, ApJ, 657, 453checked
Schwarz G. J. et al., 2007b, ApJ, 134, 516
Shara M. M., Yaron O., Prialnik D., Kovetz A., Zurek D., 2010, ApJ, **725**, 831
Starrfield S., 1989, in Bode M. F., Evans A., eds, Classical Novae, 2nd edn. Cambridge Univ. Press, Cambridge, p. 39
Starrfield S., Iliadis C., Hix W. R., 2008, in Bode M. F., Evans A., eds, Classical Novae, 2nd edn. Cambridge Univ. Press, Cambridge, p. 77
Tanaka J., Nogami D., Fuji M., Ayani K., Kato T., Maehara H., Kiyota S., Nakajima K., 2011, PASJ, 63, 911
Vanlandingham K. M. et al., 2005, ApJ, 624, 914
Walter F. M., Battisti A., Towers S. E., Bond H. E., Stringfellow G. S., 2012, PASP, 124, 1057
Warner B., 1995, Cataclysmic Variables. Cambridge Univ. Press, Cambridge
Williams S. C., Darnley M. J., Henze M., 2017, MNRAS, 472, 1300
Yamaoka H. et al., 2009, IAU Circ., 9098 #1
Yaron O., Prialnik D., Shara M. M., Kovetz A, 2005, ApJ, 623, 398

This paper has been typeset from a TEX/LATEX file prepared by the author.